Tuijin Jishu/Journal of Propulsion Technology
ISSN: 1001-4055
Vol. 45 No. 4 (2024)

Chemically Reacting Maxwell Fluid Flow to a Porous Stretching Sheet: Magnetic Field, Velocity and Concentration Slip Effects

[1]Chandu M Koli[*], [2]S.N. Salunkhe

[1]Department of Applied Science, NMIMS's SVKM Institute of Technology, Dhule, India.

[2]Department of Applied Science ,Rani Laxmibai Mahavidyalaya Parola, Jalgaon, India.

***Abstract*:** The current research objective is to employ numerical methods to observe the Maxwell fluid flow dynamics in the vicinity of a stretched surface through a chemical reaction of medium that is porous, nanoparticles, multiple slip, and magnetic field effects are influenced by convective boundary conditions. The outcome of thermophoresis and Brownian motion on the energy and concentration equations will be taken into account even as modelling the Maxwell-nanofluid flow. The dimensionless form of the fundamental governing equations is obtained through similarity transformations. The numerical solution of these dimensionless problems has been achieved through the utilisation of the Runge-Kutta technique through shooting method. This study's primary objective is to investigate key engineering factors that stem from the governing equations and their impact on profiles of temperature, concentration, and velocity. The graphic depicts an analysis of the aforementioned consequences. Furthermore, tabular formats are employed to communicate the quantitative values of diverse engineering parameters, such as skin-friction, Sherwood number, and Nusselt number coefficients. Also, a numerical comparison with previously published data at program code validation is presented

Keywords: Maxwell fluid; Magnetic field; Stretching sheet; Nanofluid; Velocity slip; Concentration slip; Chemical reaction; Runge-Kutta technique; Porous medium;

1. Introduction:

Nanofluids have been a subject of interest as cutting-edge heat transfer fluids used for approximately two decades. Despite the complex and diverse characteristics of nanofluid systems, there is currently no consensus on the magnitude of potential benefits associated with the use of heat transfer nanofluids appliances. Findings of every inquiries into heat transfer utilising nanofluids suggest that the present considerate of nanofluids remains somewhat restricted. The community of researchers studying nanofluids is faced with a range of challenges that encompass aspects such as formulation and real-world implementation, as well as gaining a deeper understanding of the fundamental mechanisms involved. The challenge of generating nanofluids among suitable particle size and morphology to enable efficient heat transfer utilisation continues to be a major hurdle in the engineering domain. Besides the influence of thermal conductivity, it is advisable for future inquiries to deem other relevant possessions, namely viscosity and wettability, and thoroughly inspect its impacts on both fluid dynamics and thermal energy transfer. A thorough

considerate of the interaction among the particles, stabilisers, the suspending medium, and the heating interface is crucial for practical applications. Nano-fluids are produced using solid particles, which can be either metallic or non-metallic. Examples of metallic solids that are commonly used include gold, silver and copper; while non-metallic solids such as alumina, silica and titanium oxide are also employed. Additionally, metallic liquids like sodium can be utilised in the production of nano-fluids. The notion of nano-fluid theory was first proposed by Choi [1] and has subsequently garnered significant attention within the field of fluid dynamics. A study was performed by Njane- Mutuku and Makinde [2] about the flowing of nanofluids above a surface that is permeable through Newtonian heating, specifically focusing on the MHD boundary layer. Behseresht [3] investigated the

influence of forces of thermophoresis & Brownian motion on the transfer of heat of nanofluids natural convection in the vicinity of an erect cone located in a drenched porous medium. Numerical data obtained through the utilisation of the Runge-Kutta method. A novel numerical methodology has been presented by Sheikholeslami [4] for analysing the flow of nanofluid MHD throughout a porous enclosure. Sheikholeslami et. al. [5] performed a research study aimed at investigating the effect of thawing transfer of heat on the augmentation of heat transfer nanofluid within an existing magnetic field. Chamkha et al. [6] observed that analysed the mixed convection boundary layer above an erect wedge situated into a porous medium. The medium was drenched through a nanofluid non-Newtonian of power law variety. Chamkha et. al. [7] looked at an investigation on the effects of lateral uniform mass flux on natural convection non-Darcy of non-Newtonian fluid with a vertical cone that is submerged into a nanofluid medium that is porous. Rashad et. al. [8] deliberated the phenomenon of hydrodynamic- magneto mixed convection contained by a square cavity that employed a lid-driven mechanism. Rashad et al. [9] examined the influence of thermophoresis and thermal radiation on the conduction of mass and heat transfer in a mixed convection scenario above an erect cone that is rotating. Sivasankaran et al. [10] conducted a study that involved a Cu-water simulation numerical mixed flow convection of nanofluid transfer of heat in a square cavity. The transfer of heat, which is turbulent, of a homogeneous nanofluid through the utilisation double twisted tapes was explored by Rokni and Sheikholeslami [11]. Muhammad etc. al. [12] examined the nanofluid 3D Eyring-Powell outcomes of thermal radiation non-linear on MHD slip, via the Cattaneo-Christov heat flux representation. Sreenivasulu et al. [13] premeditated the impact of nanofluid UCM Navier-slip effect on the flow, taking into account the influence of non-linear thermal radiation,,Lorentzian force. Zaidi et. al. [14] observed an upper-convected MHD flow of Maxwell fluid, while considering the consequence of Joule heating and convective boundary conditions, passage during erect slit. Ibrahim and Negera [15] analysed the UCM outcomes of slip on the flow performance of fluid into the occurrence of a field which is magnetic and chemical reaction. Several contemporary investigations have been conducted to evaluate the effectiveness and feasibility of nano-fluids (references [16]-[30]). The works mentioned in the literature[31]–[41] had a significant impact on understanding the nature of the reported work.References [42]-[49] provided the solutions for the MHD driven heat and mass transfer problem solving system.

The object of this study is to examine the consequence of velocity and concentration slip impact on magnetohydrodynamic nanofluid Maxwell- flow above a stretching surface, taking into consideration the existence of chemical reaction and porous medium. This research builds upon previous studies in the field. The present investigation deals with a noteworthy matter concerning the impacts of thermophoresis, Brownian motion & chemical reactions within the existence of a field that is magnetic and a porous medium. The current research problem has been addressed by employing numerical method, specifically the Runge-Kutta scheme in combination through the shooting method. The results are depicted in a graphical format, followed by a succinct analysis. The present study incorporates an analysis of specific atypical instances to establish a justification for our results. The present examination of nano-fluid is of significant importance to researchers and practitioners operating in the field of hydrodynamic fluid dynamics, specifically within the scope of lubrication theory. Thermo-bio convection, instigated by the presence of motile organisms, is a significant factor in geophysical events such as thermopiles and oil reservoirs.

2. Mathematical Construction:

In present investigate studied the characteristics of Maxwell fluid on, steady, II-dimensional incompressible, viscous electrical conducting nanofluid flow existed by surface stretching in the occurrence of a magnetic field, chemical reactions, velocity and concentration slip outcomes. The coordinate of the physical system is shown in Fig. 1. Pro this investigation, the subsequent suppositions are made:

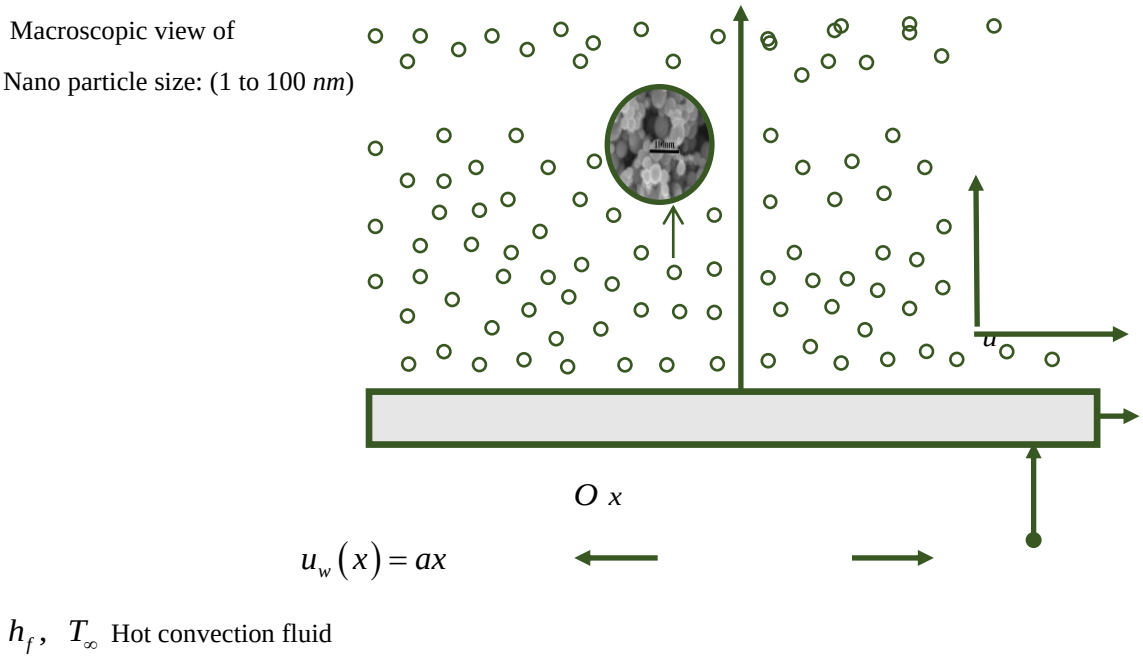

Fig. 1. Geometry depiction of the fluid

a) The geometry of the problem is supposed to be in a synchronized system where horizontal the x-axis and the y-axis is erect to it.

b) It is supposed that a nanofluid will flow steadily past a stretching sheet in a 2-dimensional (*x*, *y*) boundary layer among a linear velocity deviation with x distance and velocity slip as it wereu_w (*x*) = $ax + L_1\left(\frac{\partial u}{\partial y}\right)$.

c) Steady state of two-dimensional flows through a sheet that is stretched is taken into consideration.

d) In addition, we have measured the flow of a nanofluid in the continuation of a field that is magnetic which is normal to the nanofluid and positioned at y greater than or equal to zero; where y is the synchronized calculated normal to the stretching surface.

e) The nanoparticle volume concentration 'C'at the borders is supposed to be C_w at the wall, and C_∞ at a distance from the wall.

The equations for steady, viscous, incompressible, two-dimensional Maxwell-nanofluid boundary layer flow are provided in accordance with the presumptions as

Continuity Equation:

$$u_x + u_y = 0 \qquad (1)$$

Momentum Equation:

$$u(u_x) + v(u_y) = -\frac{1}{\rho}(p_x) + v(u_{yy}) - \left(\frac{\sigma B_0^2}{\rho}\right)u - v\left(\frac{u}{k_1}\right) - \beta\left[u^2(u_{xx}) + v^2(u_{yy}) + 2xy(u_{xy})\right] \qquad (2)$$

Equation of thermal energy:

$$u(T_x)+v(T_y)=(T_{yy})\alpha+\tau_B\left[(C_y)(T_y)D_B+\frac{D_T}{T_\infty}(T_y)^2\right] \quad (3)$$

Equation of species nanoparticle volume concentration:

$$u(C_x)+v(C_y)=(C_{yy})D_B+\left(\frac{D_T}{T_\infty}\right)(T_{yy})+Kr(C_\infty-C) \quad (4)$$

Where $\tau_B=\dfrac{(\rho C)_p}{(\rho C)_f}$.

The boundary conditions for this Maxwell-nanofluid flow with slip effects are

$$\left.\begin{array}{l} u\equiv u_w(x)=a*x+L_1(u_y), v\equiv 0, -\kappa(T_y)=(T_f-T)h_f, C\equiv C_w+L_2(C_y) \quad at \quad y\equiv 0 \\ u\to 0, v\to 0, T\to T_\infty \quad as \quad y\to\infty \end{array}\right\} \quad (5)$$

Introducing the following similarity transformations

$$\left.\psi=\sqrt{av}xf(\eta),\ \eta=y\sqrt{\frac{a}{\nu}},\ \theta=\frac{T-T_\infty}{T_f-T_\infty},\ \phi=\frac{C-C_\infty}{C_w-C_\infty}\right\} \quad (6)$$

Here ψ the stream function with $u=\dfrac{\partial\psi}{\partial y}$ & $v=-\dfrac{\partial\psi}{\partial x}$. Thus, the continuity is identically pleased. Applying the normal boundary layer approximations, an order-of-magnitude wise investigation of the momentum equation along the y-direction (perpendicular to the sheet).

$u>>v\Rightarrow u_x, v_x, v_y$ Shows that $p_x=0$ (7)

The energy, momentum, boundary condition and volume fraction (concentration) equations diminish to the pursuing set of resemblance equations when the gradient of pressure in the direction of y is disregarded.

$$f'''+ff''-Mf'-(f'^2)-Kf'-\lambda(f^2f''-2f\ f'\ f'')=0 \quad (8)$$

$$\theta''+\Pr\ f\theta'+\Pr\ Nb\theta'\phi'+\Pr\ Nt(\theta')^2=0 \quad (9)$$

$$Nb\phi''+LeNb\Pr\ f\phi'+Nt\theta''-Nb\gamma\phi=0 \quad (10)$$

The boundary conditions corresponding to (6) be

$$\left.\begin{array}{l} f(0)=0,\ f'(0)=1+\chi f''(0),\ \theta'(0)=-Bi(1-\theta(0)),\ \phi(0)=1+\delta\phi'(0) \\ f'(\infty)\to 0,\ \theta(\infty)\to 0,\ \phi(\infty)\to 0 \end{array}\right\} \quad (11)$$

Herethe physical parameters concerned are express as

$$\left.\begin{aligned} &\Pr=\frac{\nu}{\alpha},\ Le=\frac{\nu}{D_B},\ Nb=\frac{(\rho c)_p D_B(C_w-C_\infty)}{(\rho c)_f \nu},\ Nt=\frac{(\rho c)_p D_T(T_f-T_\infty)}{(\rho c)_f \nu T_\infty},\ Bi=\frac{hx}{\kappa}\sqrt{\frac{\nu}{a}},\\ &M=\frac{\sigma B_o^2}{a\rho},\ K=\frac{ak_1}{\mu},\ \chi=L_1\sqrt{\frac{a}{\nu}},\ \delta=L_2\sqrt{\frac{a}{\nu}},\ \lambda=k_o a,\ \gamma=\frac{Kr}{a}\end{aligned}\right\} \quad (12)$$

Quantities of physical interest, the physical parameters of the skin-friction coefficient, local Nusselt number and local Sherwood number are obtainable as pursues:

$$C_f=(\lambda+1)\frac{\tau_w}{\rho U_w}\Rightarrow \mathrm{Re}_x^{\frac{1}{2}}C_f=f''(0)(\lambda+1) \quad (13)$$

$$Nu_x=\frac{xq_w}{\kappa(T_w-T_\infty)} \text{ where } q_w=-\kappa\left(\frac{\partial T}{\partial y}\right)_{y=0}\Rightarrow \mathrm{Re}_x^{-\frac{1}{2}}Nu_x=-\theta'(0) \quad (14)$$

$$Sh_x=\frac{xq_m}{D_B(T_w-T_\infty)} \text{ where } q_m=-D_B\left(\frac{\partial C}{\partial y}\right)_{y=0}\Rightarrow \mathrm{Re}_x^{-\frac{1}{2}}Sh_x=-\phi'(0) \quad (15)$$

Where $\mathrm{Re}_x=\frac{U_o x}{\nu}$ be the local Reynolds number.

3. Runge-Kutta method Solutions:

A bounded domain has been substituted for the domain $[0,\ \eta_\infty]$, where η_∞ is a suitable real number, that is finite, and that needs to be chosen so that the solution gratifies the domain[0,∞) in order to solve the system of ODE's (8)-(10) numerically with their equivalent preliminary and boundary conditions (11).Additionally, the equations (8) through (10) constitute a third and second order ODE's coupled initial boundary value issue. Because of this, (8) through (10) have been condensed to a set of '7' primary problems of the first order with '7' unknowns from the hypothesis that follows in

$$f=y_1;\ f'=y_2;\ f''=y_3;\theta=y_4;\phi=y_5;\phi'=y_7.\} \quad (16)$$

As a result, we create the most efficient numerical method in accordance with the fourth order Runge-Kutta shooting technique. The numerical solution is obtained using the symbolic program MAPLE. To resolve this system, we need seven initial conditions while we have merely four initial conditions for $f(0),\ f'(0),$ $\theta(0)$ and $\phi(0)$, whereas the remaining three $f''(0),\ \theta'(0)$ and $\phi'(0)$ were not specified; therefore, we use numerical shooting technique here these three primary conditions are guessed to construct the necessary three ending boundary conditions. The step size in the mathematical simulation has to be $\Delta\eta$. = 0.001 to achieve results. The convergence criterion is$\frac{1}{10^8}$.

4. Validation of Program Code:

Table-1.: Results evaluation of Nusselt and Sherwood numbersthrough published Nusselt & Sherwood numbers results for diverse values of *Nt* as *Le.* = 10, Pr. = 10.0 and *Bi.* = 0.1.

Makinde and Aziz [49] results	current results

$-\theta'(0)_{\text{results}}$	$-\phi'(0)_{\text{results}}$	$-\theta'(0)_{\text{results}}$	$-\phi'(0)_{\text{results}}$
0.0929	2.2774	0.091765087652087	2.269567346374340
0.0927	2.2490	0.091567587567365	2.231756376375635
0.0925	2.2228	0.091686787981395	2.218678671973699
0.0923	2.1992	0.091996097304993	2.189676769376308
0.0921	2.1783	0.091946593409646	2.169689876984857

For verification of program code validation, the current Sherwood and Nusselt number results are contrasted among published Sherwood number and Nusselt number results obtained by Makinde and Aziz [50] in table-1 for $M = 0$, $K = 0$, $\lambda = 0$, $\gamma = 0$, $\chi = 0$, $\delta = 0$, for a variety of values of *Nt.* while *Le.* = 10, Pr = 10.0 and *Bi* = 0.1. From this table, it is seen that the data formed via the current code and those of Makinde and Aziz [50] show exceptional agreement and the use of the here numerical code is verified.

5. Results and Discussion:

The concentration, energy and momentum equations, along with the magnetic field, the convective boundary condition, and multiple slip effects, are used to regulate a model of non-Newtonian chemically reacting Maxwell-nanofluid flow towards a stretched sheet in this study. In order to solve the system of ODEs that are highly nonlinear and (8), (9), (10) coupled with the boundary conditions (11) that express the issue, we used the R-K approach and the shooting technique. This section's primary goal is to examine the graphical results of temperature, concentration distribution, and velocity profiles for a variety of newly discovered dimensionless parameters, including *M* –(magnetic parameter),*K* –(permeability (porosity) parameter), λ-*(*Maxwell parameter), χ -(velocity slip parameter) , *Pr*-(Prandtl number),*Nb* –(Brownian motion parameter), *Nt* -(Thermophoresis parameter), *Bi*-(Biot number), *Le*-(Lewis number),γ-(Chemical reaction parameter) and δ-(Concentration slip parameter).This section is split into two sub-sections for easier comprehension.

The values of the corresponding parameters used in the that graphical analysis are: $M = 0.5$, $K = 0.5$, $\lambda = 0.5$, Pr = 0.71, *Nb* = 0.3, *Nt* = 0.5, *Le* = 0.5, $\gamma = 0.5$, $\chi = 0.5$, *Bi* = 5.0 and $\delta = 0.5$ The velocity profiles for various values of the magnetic field parameter *(M)* are presented in Fig.2. This graphic makes it obvious that when the magnetic field parameter *(M).* is increased, the velocity reduces. The magnetic field strictures influence on the velocity profiles is slowed down by the Lorentz force, which also delays on the velocity field force. The fluid velocity and the flow's resistance are both likely to be slowed down by this force. It is therefore conceivable for the velocity profiles to drop.

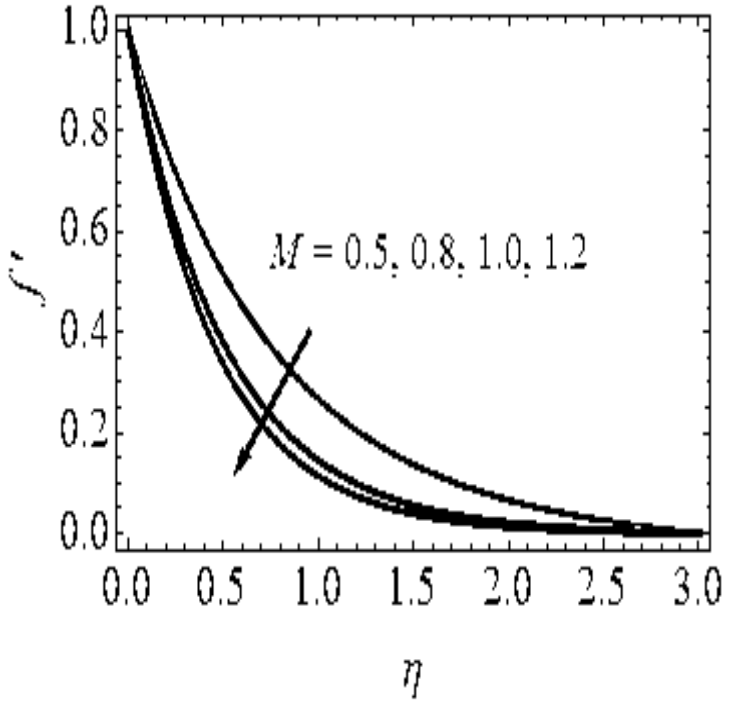

Fig. 2. Behaviour of *M* on velocity fields

Fig. 3 displays the values of the Permeability (Porosity parameter) *(K)* on velocity profiles. From this figure, additionally, it should be noted that when the parameter *K* increases, a force opposes the velocity and the boundary layer thickness.

The viscous forces between the nanofluid layers are improved by a high value of the porosity parameter in terms of physics, which reduces the fluid's momentum distribution inside the boundary layer. The Deborah number (a Maxwell fluid parameter) λ, which is a ratio of the relaxation fluid time to its characteristic scale time, has an effect on the velocity profiles, as seen in Fig. 4. The period of time during which the fluid reaches its equilibrium position after being subjected to shear stress is known as the relaxation time. For fluids with a high viscosity, this time is longer. Therefore, as illustrated in Fig. 4, an increase in λ may result in an augment in the fluid's viscosity, which will cause a drop in velocity.

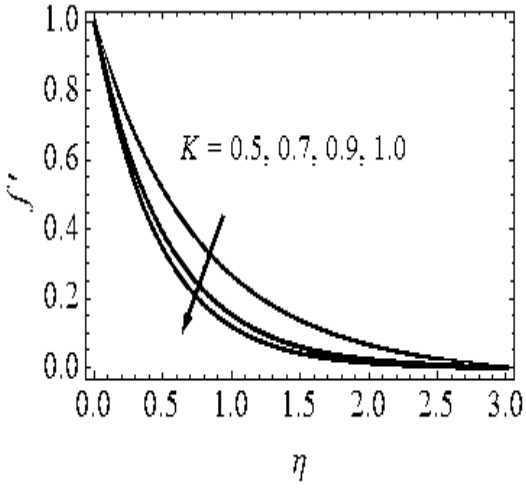

Fig. 3. Behaviour of *K* Regard velocity

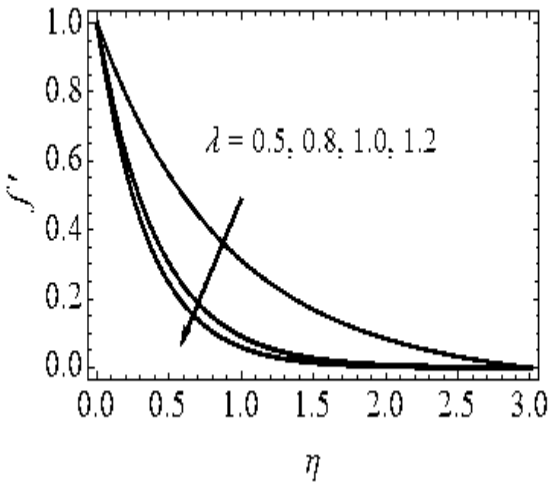

Fig. 4. Behaviour of λ Regard velocity fields

Fig. 5 described how the velocity slip ((χ)) affects the velocity. It is observed that when the velocities slip augments, the fluid's velocity drops. Prandtl number fluctuation on temperature profiles is seen in Fig.6. It is concluded that narrower temperature boundary layers are produced by increasing Prandtl number values. Temperatures drop as a result of reduced thermal diffusivity in fluids with higher Prandtl numbers.

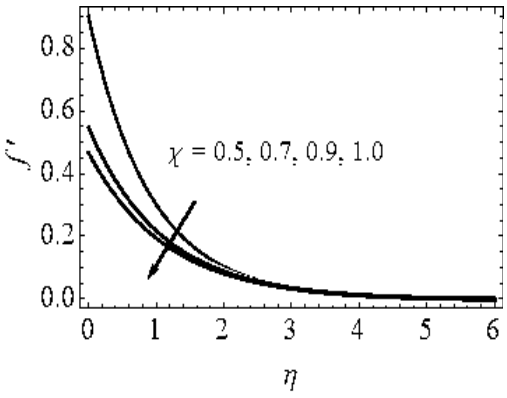

Fig. 5. Behaviour of χ Regard velocity fields

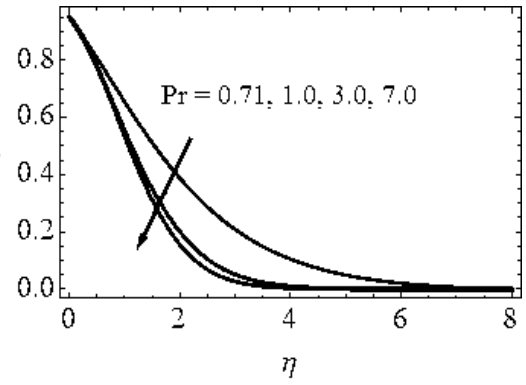

Fig. 6. Behaviour of Pr Regard temperature

Figs.7 and 8 show how the parameter of Brownian motion affects the profiles of concentration and temperature.As of the figures, it is clear that when the values of the parameter of Brownian motion climb, the thickness of the thermal boundary layer rises and the temperature differential at the surface decreases. However, when the Brownian motion parameters rise, the scientists have seen the opposite effect on the concentration profiles and thickness of concentration boundary layer.

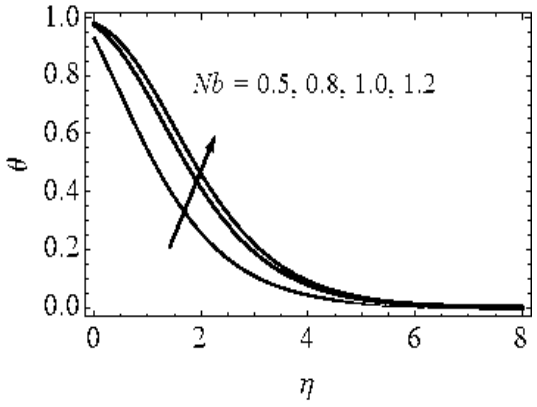

Fig. 7. Behaviour of *Nb* on temperature fields

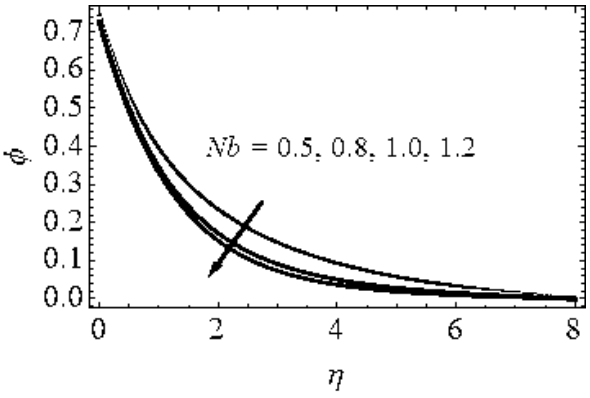

Fig. 8. Behaviour of *Nb* Regard concentration

The effects of the thermophoresis parameter on temperature and concentration silhouettes are revealed in Figs. 9 and 10. According to the figures, the temperature and concentration thickness of boundary layer improves while the thermophoresis stricture increases.

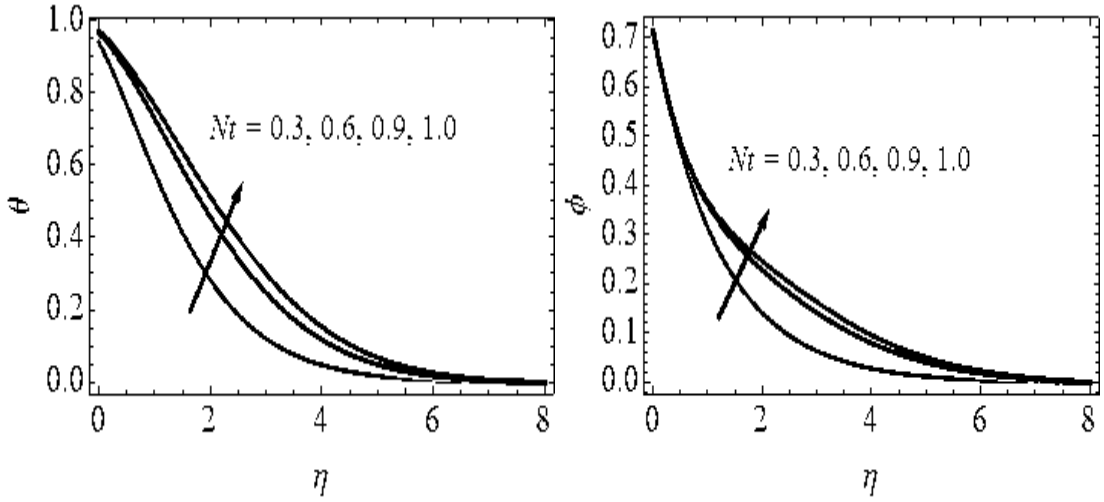

Fig. 9. Behaviour of *Nt* Regard temperature fields **Fig.10. Behaviour of *Nt* Regard concentration fields**

Fig. 11 illustrates the influence of the Biot number on temperature. It can be shown that as the number of Biots increases, so does the temperature. Figure 12 depicts the effect of the Lewis number *Le* on nanoparticle concentration profiles. It is discovered that when the Lewis number increases, the concentration drops.

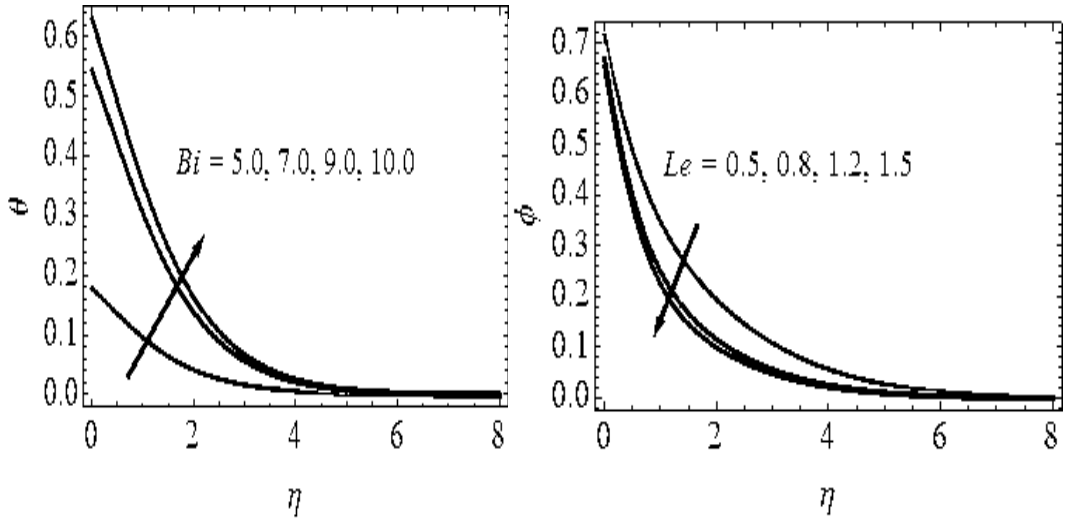

Fig. 11. Behaviour of *Bi* Regard temperature **Fig. 12. Behaviour of *Le* Regard concentration**

The persuade of the chemical reaction stricture (γ)on the nanofluid concentration (ϕ) of its nanoparticles is depicted in Fig. 13. The stronger the chemical reaction parameter value, the lower is the concentration of the nano-particle distribution (ϕ). A high rate of chemical conversion among nanofluid molecules is indicated by a large chemical reactions parameter γ , resulting in a significant delay in nanofluid concentration, as seen in the below diagram. Figure 14 depicts the fluctuation of the concentration slip parameter on dimensionless nanofluid concentration profiles. We note that the concentration profiles decreases while δ increases.

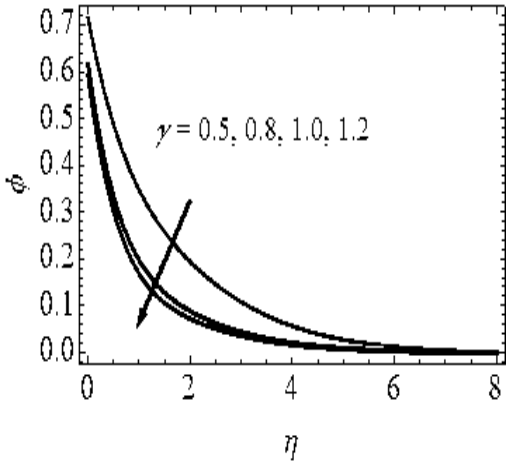

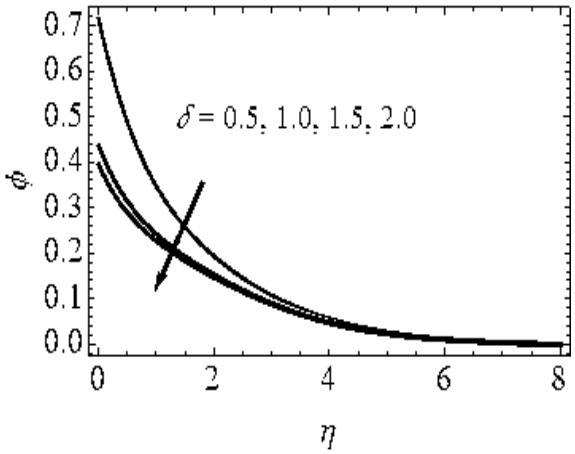

Fig. 13. Behaviour of γ Regard concentration **Fig. 14. Behaviour of δ Regard concentration**

The numerical values of Skin-friction coefficient due to velocity profiles for variations of Magnetic field parameter (M), Permeability (Porosity) parameter (K), Maxwell fluid parameter (λ), Velocity slip parameter (χ), Brownian motion parameter (Nb), Prandtl number (Pr), Thermophoresis parameter (Nt), Biot number (Bi), Lewis number (Le), Chemical reaction parameter (γ) and Concentration slip parameter (δ) are displayed in table-2. From this table, the Skin-friction coefficient values are increasing with growing values of Brownian motion parameter (Nb), (Nt)Thermophoresis parameter, (Bi) Biot number, and the numerical values of Skin-friction coefficient is decreasing with rising values of Magnetic field parameter (M), (K), Permeability (Porosity) parameter (λ)Maxwell fluid parameter, (χ)Velocity slip parameter, (Pr) Prandtl number, (Le)Lewis number, (γ.) Chemical reaction parameter, and (δ) Concentration slips parameter.

Table-2. Skin-friction coefficient results pro variations of *M, K, λ,* Pr, *Nb, Nt, Le, γ, χ, Bi*&*δ*.

M	*K*	*λ*	Pr	*Nb*	*Nt*	*Le*	*Γ*	*χ*	*Bi*	*δ*	*Cf*
0.5	0.5	0.5	0.71	0.3	0.5	0.5	0.5	0.5	5.0	0.5	2.1874530124536
0.8											2.1546343436869
1.0											2.1277582493938
	0.7										2.1686633476349
	0.9										2.1486347438077
		0.8									2.1556378373460
		1.0									2.1316642708401
			1.00								2.1434451878437
			3.00								2.1296744874380
				0.6							2.2026473834392
				0.9							2.2267474170307
					0.8						2.2186787394933
					1.0						2.2394634608742
						0.8					2.1567898196836
						1.2					2.1315674028702

							0.8				2.1676743139033
							1.0				2.1377813986234
								0.7			2.1576634780467
								0.9			2.1315674082402
									7.0		2.2164637383460
									9.0		2.2346763643086
										1.0	2.1567673763430
										1.5	2.1216768739363

The rate of heat transfer coefficient or Nusselt number values are presented in table-3 pro variations of (Pr) Prandtl number, (*Nb.*) Brownian motion parameter, (*Nt.*) Thermophoresis parameter, (*Bi.*) Biot number. At the table, it is seen that the Nusselt number values are rising with rising values of Brownian motion parameter (*Nb.*), Thermophoresis parameter (*Nt.*), Biot number (*Bi.*), and the reverse consequence is viewed in case of Prandtl number (Pr.).

Table-3. Rate of heat transfer coefficient results pro variations of *Nb*, Pr, *Nt*, &*Bi*.

Pr	*Nb*	*Nt*	*Bi*	Nu_x
0.71	0.3	0.5	5.0	1.7561396938639
1.00				1.7275317403640
3.00				1.7078768183967
	0.6			1.7875738734783
	0.9			1.8078789481892
		0.8		1.7998719786897
		1.0		1.8116547387845
			7.0	1.7965763783641
			9.0	1.8206398463961

The Sherwood number or rate of mass transfer coefficient due to concentration profiles for variations of *Nb*-(Brownian motion parameter), δ – (Concentration slip parameter), γ – (Chemical reaction parameter), *Le*-(Lewis number) and *Nt*-(Thermophoresis parameter) numerical values are displayed in table-4. From this table, the Sherwood number values are decreasing with riseing values of *Le*-(Lewis number), *Nb*-(Brownian motion parameter), δ –(Concentration slip parameter), γ –(Chemical reaction parameter), while the Sherwood number values are increasing with rising values of *Nt* –(Thermophoresis parameter).

Table-4. Skin-friction coefficient results for variations of *Le*, *Nb*, *Nt*, γ, &δ.

Nb	*Nt*	*Le*	γ	Δ	Sh_x
0.3	0.5	0.5	0.5	0.5	1.9678719386983
0.6					1.9488168979181
0.9					1.9215673468659
	0.8				1.9878498187367

	1.0				2.0867847597199
		0.8			1.9277548185971
		1.2			1.8977888738768
			0.8		1.9377489304730
			1.0		1.9115643762304
				1.0	1.9463738368063
				1.5	1.9215674362076

6. Conclusions:

In this research investigation, the authors have to examine the outcomes of two-dimensional, steady, conducting electrically, incompressible, Maxwell non-Newtonian fluid flow in addition of nanofluid particles towards a stretching sheet surrounded by porous medium in the occurrence of slip Velocity, Magnetic field, Concentration slip along with effects of Brownian motion & Thermophoresis. Numerical results were found and discussed by graphical and numerical solutions with the Runge-Kutta process and shooting method are used. The investigation's findings as below

- In the occurrence of the Magnetic field parameter, the velocity profiles are reduced.
- Decreases in velocity are observed for the Permeability and slip Velocity parameters.
- The velocity profile diminishes in the presence of the Maxwell fluid stricture.
- Various parameters in the Maxwell-Nanofluid flow Temperature distribution increase as Brownian motion, Thermophoresis parameters are increased.
- The temperature silhouette diminishes in the presence of the Prandtl number.
- When Biot number is enhanced, the temperature profiles are enhanced as well.
- The concentration silhouettes decrease with increasing Lewis number; Brownian motion stricture, Chemical reaction stricture & Concentration slip parameter.
- The concentration silhouettes are increases with Thermophoresis parameter values are increased.
- This study might be broadened to include non-Newtonian nanofluids such as those included by Williamson and Jeffrey, the constricted vein in the elliptical cross-section, and several other types under different physical circumstances.
- In program code validation, the acquire results be good agreement among the published results of Makinde and Aziz [50].

References:

[1] S. Choi, Developments and applications of non-newtonian flows, vol. 66 (1995), pp. 99-105.

[2] W. N. Mutuku-Njane, O. D. Makinde, On hydromagnetic boundary layer flow of nanofluids over a permeable moving surface with newtonian heating, Latin Am. Appl. Res., 44 (2014), pp. 57-62.

[3] A. Behseresht, A. Noghrehabadi, M. Ghalambaz, Natural-convection heat and mass transfer from a vertical cone in porous media filled with nanofluids using the practical ranges of nanofluids thermo-physical properties, Chem. Eng. Res. Des., 92 (3) (2014), pp. 447-452, 10.1016/j.cherd.2013.08.028.

[4] M. Sheikholeslami, Numerical approach for MHD Al_2O_3-water nanofluid transportation inside a permeable medium using innovative computer method, Comput. Methods Appl. Mech. Eng., 344 (2019), pp. 306-318.

[5] M. Sheikholeslami, M. K. Sadoughi, Simulation of CuO-water nanofluid heat transfer enhancement in presence of melting surface, Int. J. Heat Mass Transf., 116 (2019), pp. 909-919.

[6] A. J. Chamkha, A. M. Rashad, R. S. R. Gorla, Non-similar solutions for mixed convection along a wedge embedded in a porous medium saturated by a non-newtonian nanofluid: natural convection dominated regime, Int. J. Numer. Meth. Heat Fluid Flow, 24 (5) (2014), pp. 1471-1786.

[7] J. Chamkha, A. M. Saeid Abbasbandy, Rashad, Non-Darcy natural convection flow of a non-newtonian nanofluid over a cone saturated in a porous medium with uniform heat and volume fraction fluxes, Int. J. Numer. Meth, Heat Fluid Flow, 25 (2) (2015), pp. 422-437.

[8] M. Rashad, Muneer A. Ismael, Ali J. Chamkha, M. A. Mansour, MHD mixed convection of localized heat source/sink in a nanofluid-filled lid-driven square cavity with partial slip, J. Taiwan Inst. Chem. Eng., 68 (2016), pp. 173-186.

[9] M. Rashad, B. Mallikarjuna, A. J. Chamkha, S. Hariprasad Raju, Thermophoresis effect on heat and mass transfer from a rotating cone in a porous medium with thermal radiation, Afrika Matematika, 27 (2016), pp. 1409-1424.

[10] M. Sivasankaran, M. A. Mansour, A. M. Rashad, M. Bhuvaneswari, MHD Mixed convection of cu-water nanofluid in a two-sided lid-driven porous cavity with a partial slip, Numer. Heat Transfer Part A, 70 (12) (2016), pp. 1356-1370.

[11] M. Sheikholeslami, M. Jafaryar, Ahmad Shafee, Zhixiong Li, Rizwan-ul Haq, Heat transfer of nanoparticles employing innovative turbulator considering entropy generation, Int. J. Heat Mass Transf., 136 (2019), pp. 1233-1240.

[12] T. Muhammad, H. Waqas, S. A. Khan, R. Ellahi, S. M. Sait, Significance of nonlinear thermal radiation in 3D Eyring–Powell nanofluid flow with Arrhenius activation energy, J. Therm. Anal. Calorim., 143 (2021), pp. 929-944.

[13] P. Sreenivasulu, T. Poornima, B. Vasu, R. S. R. Gorla, N. B. Reddy, Non-linear radiation and Navier-slip effects on UCM nanofluid flow past a stretching sheet under Lorentzian force, J. Appl. Comput. Mech., 7 (2) (2021), pp. 638-645.

[14] Z. A. Zaidi, S. T. Mohyud-Din, Effect of Joule heating and MHD in the presence of convective boundary condition for upper convected Maxwell fluid through wall jet, J. Mol. Liq., 230 (2017), pp. 230-234.

[15] W. Ibrahim, M. Negera, MHD slip flow of upper-convected Maxwell nanofluid over a stretching sheet with chemical reaction, J. Egypt. Math. Soc., 28 (7–34) (2020).

[16] T. Muhammad, H. Waqas, U. Farooq, M. S. Alqarni, Numerical simulation for melting heat transport in nanofluids due to quadratic stretching plate with nonlinear thermal radiation, Case Stud. Therm. Eng., 27 (2021), Article 101300.

[17] M. R. Eid, K. L. Mahny, T. Muhammad, M. Sheikholeslami, Numerical treatment for Carreau nanofluid flow over a porous nonlinear stretching surface, Results Phys. (2018), pp. 1185-1193.

[18] S. M. Atif, S. Hussain, M. Sagheer, Effect of viscous dissipation and Joule heating on MHD radiative tangent hyperbolic nanofluid with convective and slip conditions, J. Braz. Soc. Mech. Sci. Eng., 41 (4) (2019), pp. 189-206.

[19] S. M. Atif, S. Hussain, M. Sagheer, Heat and mass transfer analysis of time dependent tangent hyperbolic nanofluid flow past a wedge, Phys. Lett. A, 383 (11) (2019), pp. 1187-1198.

[20] M. Hamid, M. Usman, Z. H. Khan, R. U. Haq, W. Wang, Numerical study of unsteady MHD flow of Williamson nanofluid in a permeable channel with heat source/sink and thermal radiation, Eur. Phys. J. Plus, 133 (2018), p. 527.

[21] M. Usman, M. Hamid, U. Khan, S. T. M. Din, M. A. Iqbal, W. Wanga, Differential transform method for unsteady nanofluid flow and heat transfer, Alex. Eng. J., 57 (3) (2018), pp. 1867-1875.

[22] S. Shah, S. Hussain, M. Sagheer, M. Bilal, Numerical study of three dimensional mixed convective Maxwell nanofluid flow over a stretching surface with non-linear thermal radiation and convective boundary conditions, J. Nanofluids, 8 (1) (2018), pp. 160-170.

[23] T. Hayat, T. Muhammad, A. Qayyum, A. Alsaedi, M. Mustafa, On squeezing flow of nanofluid in the presence of magnetic field effects, J. Mol. Liq., 213 (2016), pp. 179-185.

[24] M. Sagheer, S. Shah, S. Hussain, M. Akhtar, Impact of non-uniform heat source/sink on magnetohydrodynamic Maxwell nanofluid flow over a convectively heated stretching surface with chemical reaction, J. Nanofld, 8 (4) (2019), pp. 795-805.

[25] T. Muhammad, S.Z. Alamri, H. Waqas, D. Habib, R. Ellahi, Bio-convection flow of magnetized Carreau nanofluid under the influence of slip over a wedge with motile microorganisms, J. Therm. Anal. Calorim., 143 (2021), pp. 945-957.

[26] S. Shah, S. M. Atif, A. Kamran, Radiation and slip effects on MHD Maxwell nanofluid flow over an inclined surface with chemical reaction, Heat Trans. J. (2021).

[27] M. K. Nayak, S. Shaw, H. Waqas, O. D. Makinde, M. Alghamdi, T. Muhammad, Comparative study for magnetized flow of nanofluids between two parallel permeable stretching/shrinking surfaces, Case Stud. Therm. Eng., 28 (2021), Article 101353.

[28] P. M. Kumar, C. A. Kumar, Numerical study on heat transfer performance using Al2O3/water nanofuids in six circular channel heat sink for electronic chip, Mater. Today, Proc., 21 (2020), pp. 194-201.

[29] W. Ibrahim, M. Negera, Melting and viscous dissipation effect on upper-convected Maxwell and Williamson nanofluid, Eng. Rep., 2 (5) (2020).

[30] G. V. Lakshmi, L. A. Babu, K. S. Rao, MHD mixed convection stagnation point flow of nanofluid through a porous medium over stretching sheet, Int. J. Pure Appl. Math., 118 (10) (2018), pp. 369-389.

[31] G Murali, A Paul, NVN Babu,Heat and mass transfer effects on an unsteady hydromagnetic free convective flow over an infinite vertical plate embedded in a porous medium with heat absorption, *Int. J. Open Problems Compt. Math* 8 (1), 2015.

[32] Deepa Gadipally,Murali Gundagani,Analysis of soret and dufour effects onunsteady MHD flow past a semi infinite vertical porous plate via finite difference method, *International journal of applied physics and mathematics*,4(5),332-344,2014.DOI: 10.7763/IJAPM.2014.V4.306.

[33] G.Murali,Ajit Paul, NVN Babu,Numerical study of chemical reaction effects on unsteady MHD fluid flow past an infinite vertical plate embedded in a porous medium with variable suction, *Electronic Journal of mathematical analysis and applications*,3(2),179-192,2015.

[34] NVN Babu, Ajit Paul,G Murali, Soret and Dufour effects on unsteady hydromagnetic free convective fluid flow past an infinite vertical porous plate in the presence of chemical reaction, *Journal of science and arts*,15 (1), pp. 99-111, 2015.

[35] Murali Gundagani, MCK Reddy,Sivaiah (2012) Finite element solution of thermal radiation effect on unsteady MHD flow past a vertical porous plate with variable suction,*American Academic & Scholarly Research Journal* 4 (3), 3-22,2012.

[36] Babu, N.V.N.,Murali, G., Bhati, S.M.(2018). Casson fluid performance on natural convective dissipative couette flow past an infinite vertically inclined plate filled in porous medium with heat transfer, MHD and hall current effects, *International journal of Pharmaceutical Research, 10*(4), 2018.

[37] M. Gundagani, S. Sheri, A. Paul, and M. C. K. Reddy, "Radiation Effects on an Unsteady MHD Convective Flow Past a Semi-Infinite Vertical Permeable Moving Plate Embedded in a Porous Medium with Viscous Dissipation", *Walailak J Sci &; Tech*, vol. 10, no. 5, pp. 499–515, Apr. 2013.

[38] Murali Gundagani, Sivaiah Sheri , Ajit Paul , and M. C. K. Reddy Unsteady magnetohydrodynamic free convective flow past a vertical porous plate, *International journal of applied science and engineering*, vol. 11, no. 3, pp. 267–275, 2013.

[39] G. Murali1 , G. Deepa, Nirmala Kasturi V , T. Poornakantha (2023),Joint effects of thermal diffusion and diffusion thermo on MHD three dimensional nanofluid flow towards a stretching sheet, *Mathematical models in engineering*, DOI https://doi.org/10.21595/mme.2023.23590.

[40] Gundagani, M., Babu, N.V.N., Gadially, D. *et al.* Study of Nano-Powell-Erying fluid flow past a porous stretching sheet by the effects of MHD, thermal and mass convective boundary conditions. *J. Umm Al-Qura Univ. Eng. Archit.* (2024). https://doi.org/10.1007/s43995-024-00056-2

[41] S.M.Bhati,G.Murali,Ch.Sanjay, Law of Magnetic Fields Via Bianchi Identities, *Journal of Applied Science and Engineering*, 25(4),2024,https://doi.org/10.6180/jase.202208_25(4).0011.

[42] Gundagani, M., Mamidi, L.P. & Tanuku, P.K. Finite element solutions of Double diffusion effects on three-dimensional MHD Nano-Powell-Erying fluid flow in presence of thermal and mass Biot numbers. *J. Eng. Appl. Sci.* 71, 9 (2024). https://doi.org/10.1186/s44147-023-00347-w

[43] G Deepa, G Murali, Effects of viscous dissipation on unsteady MHD free convective flow with thermophoresis past a radiate inclined permeable plate,*Iranian Journal of Science and Technology (Sciences)*, 38A3, 2014. DOI: 10.22099/IJSTS.2014.2437

[44] Murali G, NVN Babu, Convective MHD Jeffrey Fluid Flow Due to Vertical Plates with Pulsed Fluid Suction:A Numerical Study,*Journal of computational applied mechanics* DOI *10.22059/JCAMECH.2023.351326.773,2023.*

[45] G Murali, NVN Babu, Effect of Radiation on MHD Convection Flow Past a Vertical Permeable Moving Plate, *International Journal of Advances in Applied Sciences*(IJAAS),2012,Vol.1, No.1, March 2012, pp. 19~28,ISSN: 2252-8814.

[46] S.Sivaaih,G.Murali, MCK Reddy,R.Srinivasa Raju,Unsteady MHD mixed convection flow past a vertical porous plate in prsesence of radiation, *International journal of basic and applied sciences*, 1(4),651-666,2012.

[47] MCK Reddy, G Murali, S Sivaiah, NVN Babu, Heat and mass transfer effects on unsteady MHD free convection flow past a vertical permeable moving plate with radiation, *International Journal of Applied Mathematical Research*, 1 (2) (2012),189-205.

[48] S Sivaiah, G Murali, MCK Reddy,Finite Element Analysis of Chemical Reaction and Radiation Effects on Isothermal Vertical Oscillating Plate with Variable Mass Diffusion,International Scholarly Research Network ISRN Mathematical Physics Volume 2012, Article ID 401515, doi:10.5402/2012/401515.

[49] Murali Gundagani,S Sheri, MCK Reddy,Soret and dufour effects on unsteady mhd mixed convection flow past a verticle porous plate with thermal radiation,*Caspian journal of applied sciences research*,1(9),2012.

[50] Makinde O. D., Aziz A.(2011), Boundary layer flow of a nanofluid past a stretching sheet with a convective boundary condition. Int. J. Therm. Sci.,Vol. 50, pp. 1326-1332.